



Lawrence Berkeley Laboratory

UNIVERSITY OF CALIFORNIA

RECEIVED
LAWRENCE
BERKELEY LABORATORY
APR 16 1981
LIBRARY AND
DOCUMENTS SECTION

Submitted to Physics Letters

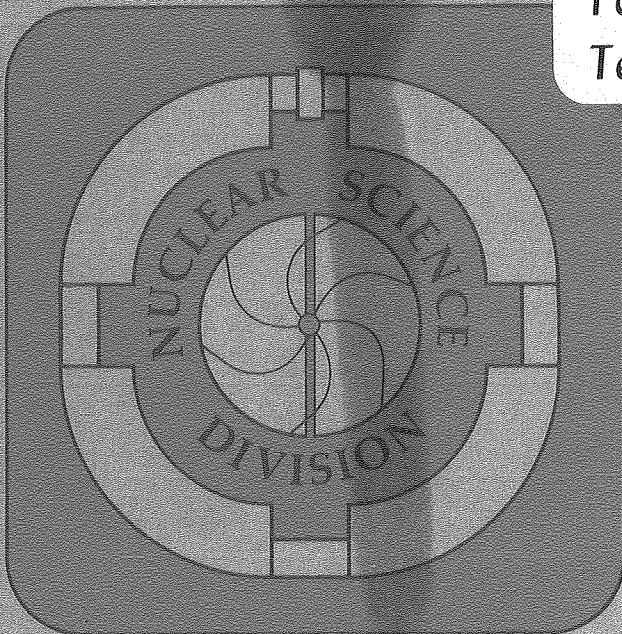
PROBING DENSE NUCLEAR MATTER VIA NUCLEAR COLLISIONS

H. Stöcker, M. Gyulassy and J. Boguta

January 1981

TWO-WEEK LOAN COPY

*This is a Library Circulating Copy
which may be borrowed for two weeks.
For a personal retention copy, call
Tech. Info. Division, Ext. 6782*



*LBL-12095
c.2*

DISCLAIMER

This document was prepared as an account of work sponsored by the United States Government. While this document is believed to contain correct information, neither the United States Government nor any agency thereof, nor the Regents of the University of California, nor any of their employees, makes any warranty, express or implied, or assumes any legal responsibility for the accuracy, completeness, or usefulness of any information, apparatus, product, or process disclosed, or represents that its use would not infringe privately owned rights. Reference herein to any specific commercial product, process, or service by its trade name, trademark, manufacturer, or otherwise, does not necessarily constitute or imply its endorsement, recommendation, or favoring by the United States Government or any agency thereof, or the Regents of the University of California. The views and opinions of authors expressed herein do not necessarily state or reflect those of the United States Government or any agency thereof or the Regents of the University of California.

Probing Dense Nuclear Matter via
Nuclear Collisions*

H. Stöcker, M. Gyulassy and J. Boguta

Nuclear Science Division
Lawrence Berkeley Laboratory
University of California
Berkeley, CA 94720

Abstract

We study the sensitivity of nuclear hydrodynamics to the equation of state of nuclear matter at high densities and temperatures. The pressure, P , and entropy, S , generated in nuclear collisions between 50 and 2000 MeV/nucleon are computed in a variety of models for the equation of state. The high precision required in jet and composition analysis to deduce P and S from data is discussed.

*This work was supported by the Director, Office of Energy Research, Division of Nuclear Physics of the Office of High Energy and Nuclear Physics of the U.S. Department of Energy under Contract W-7405-ENG-48 and by Deutscher Akademischer Austausch Dienst (DAAD), Bonn, West Germany.

Nuclear collisions at high energies offer a unique opportunity in the laboratory for probing the properties of nuclear matter at high densities, ρ , and temperatures, T . Experimental evidence for preferential sideways emission of matter in nearly central collisions¹⁻³ has been interpreted^{4,5} as being due to the collective flow of shocked nuclear matter during the compression and expansion stages of the collision. The observed large transverse momentum transfer on heavy target residues^{3,6,7} can be interpreted in the bounce off model^{4,5,8} as consequence of the large pressure in the shock zone exerted on the "spectator" fragments. The validity of such a fluid dynamical interpretation^{9,10} of nuclear collisions requires, however, that the nucleon mean free path, $\lambda \sim 2$ fm, is much smaller than the size of the system $R \approx 1.2 A^{1/3}$ fm. In practice¹¹, $R/\lambda \gtrsim 3$ ($A \gtrsim 125$) insures local thermal equilibration, the prerequisite for hydrodynamics. Thus far only light nuclear beams ($A < 40$) were available experimentally, and indeed evidence for nonequilibrium dynamics has been observed in collisions of light, equal mass nuclei¹². In the near future, beams up to uranium will be available, for which such nonequilibrium, finite particle effects are expected to be much less important.

Assuming then that fluid dynamics is valid at least for not too peripheral collisions of heavy nuclei, the important question is how sensitive are the predicted observables to the nuclear matter equation of state, $W(\rho, T)$ = energy per nucleon at a given density, ρ , and temperature, T . In other words, what are our chances for deducing $W(\rho, T)$ experimentally?

Previous calculations assuming chemical equilibration have shown that hadron (π, Δ) production¹³⁻¹⁵ excitation functions and light (p, d, He) nuclear fragment ratios^{15,16} yield $\sim 50\%$ sensitivity to the nuclear equation of state. However, calculations using hadron chemistry¹⁷ cast doubt

on full chemical equilibration, and thus the sensitivity of those ratios to $W(\rho, T)$ would be even less.

Numerical calculations of double differential inclusive cross section, $d^2\sigma/d\Omega dE$, have shown no significant sensitivity to the compression part $W_c(\rho)$, of $W(\rho, T)$, at the level of the $\lesssim 50\%$ numerical uncertainties.^{10,13,15,18-20} It was shown^{4,5}, however, that the sensitivity of double differential cross sections, $d^2\sigma/d\Omega dE$, on the reaction dynamics could be increased by detailed inspection of (1) triple differential cross sections⁵, $d^3\sigma/dE d\cos\theta d\phi$, of the various emitted particles and (2) the predicted jets^{4,5} of matter to be observed in 4π exclusive data analysis. In this paper, we show analytically that the level of sensitivity to $W_c(\rho)$ of the average fluid dynamical behavior can be understood from the Rankine-Hugoniot equation.^{2,9,10} Specifically, we calculate the maximum pressure, $P(E) = P[\rho(E), T(E)]$, and the entropy per nucleon, $S(E) = S[\rho(E), T(E)]$, as a function of the beam kinetic energy per nucleon, E , by using the relativistic Rankine-Hugoniot equation to estimate $\rho(E)$ and $T(E)$. Unlike $W(\rho, T)$, $P(E)$ and $S(E)$ can be directly related to experimental observables: The pressure, as the driving force for the fluid motion, determines the mean collective flow behavior, especially the transverse momentum transfer^{4,8}, while the entropy produced determines the hadron production rates¹³⁻¹⁵ and chemical composition of light nuclear fragments.^{15,16}

At present, the combined measurement of $P(E)$ and $S(E)$ via detailed jet analysis and composition analysis promises in fact the best prospects for determining $W(\rho, T)$ ultimately from nuclear collision data.^{21,22}

We start with the Rankine-Hugoniot equation^{2,9,10},

$$(W^2 - W_0^2) + P(W/\rho - W_0/\rho_0) = 0, \quad (1)$$

since shock formation is the primary mechanism for compression and entropy production in hydrodynamics at these energies. Furthermore, the maximum densities and temperatures achieved in full 3D hydrodynamical calculations agree well^{9,10} with those expected from eq. (1). This is natural since eq. (1) simply expresses conservation of baryon, momentum, and energy fluxes across the shock front. On one side of the shock, normal nuclear matter with $\rho = \rho_0 = 0.17 \text{ fm}^{-3}$ and $T = 0$ is streaming inwards uniformly. On the other side of the shock, hot, compressed nuclear matter with $\rho > \rho_0$, $T > 0$ is formed. Eq. (1) is derived in the frame in which the compressed matter has zero flow velocity. The energy per nucleon, $W(\rho, T)$, in the shock zone is therefore fixed by the lab kinetic energy per nucleon E as

$$W = \gamma_{\text{cm}}(E)W_0, \quad (2)$$

where $W_0 = m_N - B \approx 931 \text{ MeV}$ and $\gamma_{\text{cm}} = (1 + E/2W_0)^{1/2}$. Note that eqs. (1,2) can be applied only up to the time when the smaller nucleus is consumed by the shock zone. After that time the shock zone can no longer be maintained by the incoming streaming matter, and the compressed matter expands nearly isentropically^{9,10,16}.

Usually^{2,9,10}, eq. (1) is solved to obtain $\rho(E)$ and $T(E)$ in the compressed region. However, we observe that with eqs. (1,2) the total pressure $P(E)$ in the shock is given simply by

$$P(E) = \frac{1}{2} E \rho_0 [1 - \gamma_{\text{cm}}(E) \rho_0 / \rho(E)]^{-1}. \quad (3)$$

Eq. (3) shows that the only source of sensitivity of $P(E)$ to $W(\rho, T)$ occurs through the dependence of $\rho(E)$ on W . Unfortunately, the higher the compression achieved, the weaker is the dependence of $P(E)$ on W !

To illustrate this weak dependence on W , consider first the case when there is no compression energy ($W_c = 0$) and $P = P_T$, where

$$P_T(\rho, T) = \alpha \rho W_T(\rho, T) \quad . \quad (4)$$

For $\alpha = 2/3$, eq. (4) corresponds to the nonrelativistic ideal or Fermi gas equation of state. Regardless of the form of $W_T(\rho, T)$, W_T is constrained by eq. (2) to be

$$W_T[\rho(E), T(E)] = (\gamma_{cm}(E) - 1)W_o \quad . \quad (5)$$

With eqs. (4,5), eq. (1) yields

$$\begin{aligned} \rho(E) &= \rho_o \{ (1 + \alpha) \gamma_{cm}(E) + 1 \} / \alpha \\ &\approx \frac{2 + \alpha}{\alpha} \left\{ 1 + \frac{1 + \alpha}{2 + \alpha} \frac{E}{4W_o} \right\} \rho_o, \end{aligned} \quad (6)$$

and

$$\begin{aligned} P(E) &= W_o \rho_o \{ (1 + \alpha) \gamma_{cm}(E) + 1 \} \{ \gamma_{cm}(E) - 1 \} \\ &\approx \frac{1}{2} E \rho_o \left(1 + \frac{\alpha}{2} \right) \quad , \end{aligned} \quad (7)$$

where the approximate forms hold for $E \lesssim 1$ GeV/nucleon. It is instructive to consider three cases, $\alpha = 1/3, 2/3, 1$, corresponding to soft, normal, and stiff thermal equations of state. For a fixed density ρ and E , $P(E)$ varies by a factor of three in this range of α . However, eq. (1) only allows a specific $\rho = \rho(E)$, eq. (6) for a given α and E . For $E \lesssim 1$ GeV/nucleon, $\rho(E)/\rho_o \sim 7, 4, 3 \rho_o$ for $\alpha = 1/3, 2/3, 1$, respectively. Therefore, rather different densities are achieved for the three different equations of state. Nevertheless, $P(E)/(E\rho_o/6) = 7, 8, 9$, respectively, showing that the total pressure differs by $\sim 30\%$!

We next study the effect of including a compression energy $W_c(\rho)$. The following popular^{9,10,15,20} functional forms were tested:

$$W_c(\rho) = \begin{cases} K(\rho - \rho_0)^2/18\rho\rho_0 & , & (8a) \\ K(\rho - \rho_0)^2/18\rho_0^2 & , & (8b) \\ 2K(\sqrt{\rho/\rho_0} - 1)^2/9 & , & (8c) \\ K(\rho_0/\rho - 1 + \ln\rho/\rho_0)/9 & , & (8d) \end{cases}$$

where $K = 9\rho_0^2 d^2 W_c / d^2 \rho_0$ is the incompressibility modulus. For a given $W_c(\rho)$, the pressure due to compression is just $P_c(\rho) = \rho^2 dW_c / d\rho$. We assume the thermal pressure is given by eq. (4). Eq. (1) can then be solved analytically for $\rho(E)$ and $P(E)$. In order to compare the various cases, we plot the ratio, $P(E)/P_{FG}(E)$, where the Fermi gas pressure is given by eq. (7) with $\alpha = 2/3$.

In Fig. 1a, we vary K from 100 to 800 MeV for a fixed functional form of $W_c(\rho)$ given by eq. (8a). In Fig. 1b, we fix $K = 200$ MeV but vary the functional form of $W_c(\rho)$ via eqs. (8a-8d). In Fig. 1c, we fix $K = 200$ MeV and $W_c(\rho)$ with eq. (8a) but now vary the thermal part via $\alpha = 1/3, 2/3, 1$ in eq. (4). For the equations of state considered in Fig. 1 we also show in Fig. 2 the corresponding ratio of the compression pressure to the thermal pressure P_c/P_T . The absolute value of the Fermi gas pressure is plotted in Fig. 3a. In addition, in Fig. 3a we compare P_{FG} to realistic equations of state based on relativistic mean field theory^{23,24}. The pressures in those theories are given in terms of the self-consistent scalar, σ , and vector, V_0 , fields [see Refs. (23,24) for details].

The predicted almost linear increase of P with E is of interest, as it may be used to determine the low and high energy limits of the validity of the fluid dynamical treatment, e.g. via measurements of the transverse momentum transfer⁸. In this context, the large absolute values of P at high energies ($P \gtrsim 150 \text{ MeV/fm}^3$ at $E = 1 \text{ GeV/n}$) for all the equations of state considered should also be emphasized.

The important observation, in accord with eq. (3), is that as E increases, $\rho(E)$ increases (Fig. 3c), and $P(E)$ is less sensitive to variations in $W_c(\rho)$, while the sensitivity to W_T increases.

The maximum sensitivity ($\sim 50\%$) to the compression part of W occurs for $E \sim 50\text{--}100 \text{ MeV/nucleon}$. There is clearly a lower bound of $E \gtrsim 50 \text{ MeV/nucleon}$ below which hydrodynamics cannot apply due to Pauli blocking, and mean field dynamics (TDHF) is appropriate²⁵. Therefore, $E \sim 100 \text{ MeV/nucleon}$ seems to be most promising in gaining sensitivity to W_c . At higher energies ($E > 1 \text{ GeV/nucleon}$), $P_T > P_c$ (see Fig. 2) and there is very little sensitivity to P_c . On the other hand, at these higher energies, the sensitivity to P_T increases, but again only to $\sim 25\%$ when α is varied from $1/3$ to 1 . Therefore, at high energies $E > 1 \text{ GeV/nucleon}$, rather high precision measurement of $P(E)$ (via jet analysis⁵) must be made in order to distinguish between various $W_T(\rho, T)$. We emphasize that the insensitivity of $P(E)$ to W is not due to a too restrictive choice of functional forms of $W(\rho, T)$. As seen in Fig. 2, the ratio of P_c/P_T varies by a factor of 10 as W_c and W_T are varied. However, the sum, $P = P_c + P_T$, which is the driving force of hydrodynamics, varied by only 30% above a few hundred MeV/nucleon! Baryon and energy-momentum conservation, eq. (3), are such strong constraints on P that the details of exactly how the energy is partitioned into compression and thermal parts lead to $\sim 30\%$ corrections only.

Next we turn to entropy production. For $P_T = \rho^2 \partial W_T / \partial \rho|_S$ of the form eq. (4), we must have $W_T(\rho, S) = f(S)(\rho/\rho_0)^\alpha$. For illustration we consider $f(S) \propto S^2$, as in the degenerate Fermi gas case, implying $W_T \propto T^2/\rho^\alpha$. In this case,

$$S(E) = C[W_T(E)/W_0]^{1/2} [\rho_0/\rho(E)]^{\alpha/2} . \quad (9)$$

For the degenerate Fermi gas case with no compression energy, we get via eqs. (5,6)

$$S_{FG}(E) \approx 4.9(E/m_N)^{1/2} . \quad (10)$$

Therefore, we set $C = 15.5$ so that eq. (9) coincides with eq. (10) when $\alpha = 2/3$ and $E/m_N \ll 1$. We note that the exact Fermi gas entropy is somewhat less than eq. (10) as seen in Fig. 3b. However, for our purposes eq. (9) will suffice to illustrate the sensitivity of $S(E)$ to $W(\rho, T)$.

In Fig. 1 we plot $S(E)/S_{FG}(E)$ for the variety of equations of state discussed. In Fig. 1a, 1b, $\alpha = 2/3$ is used in eq. (9). In Fig. 1c, eq. (9) with $\alpha = 1/3, 2/3, 1$ including compression [eq. (8a)] are compared to eq. (10). Note that the $\alpha = 2/3$ case is not equal to S_{FG} because in Fig. 1c the compression energy eq. (8a) modifies the W_T and ρ entering eq. (9). The entropy $S_{MF}(E)$ in the self-consistent mean field theory^{23,24} is compared to the exact S_{FG} on an absolute scale in Fig. 3b. Note that S_{MF} reduces to the exact Fermi gas entropy when the scalar and vector interactions are reduced. The absolute values of $S(E)$ can be compared to those extracted¹⁶ from measured d/p ratios.

As with $P(E)/P_{FG}(E)$, $S(E)/S_{FG}(E)$ is most sensitive to W_c at lower energies ~ 100 MeV/nucleon. However, a factor of eight variation of K again leads to a $\sim 20\%$ variation of $S(E)$ in Fig. 1a only. The variation of W_T via $\alpha = 1/3$ to 1 leads also to a $\sim 30\%$ variation in $S(E)$ at higher energies ~ 1 GeV/nucleon only. In Fig. 1a we can see that for a fixed functional form of W_c , eq. (8a), $S(E)$ decreases with increasing incompressibility K . However, in Fig. 1b, for a fixed $K = 200$ increasing the compression energy at high ρ by using the stiffer eq. (8b) instead of eq. (8a) leads to an increase in the entropy.

This previous observation shows the importance of measuring both $P(E)$ and $S(E)$, if $W_c(\rho)$ is to be ultimately determined. For example, for $E = 100$ MeV/nucleon $P/P_{FG} \approx 1.4$ for either $K = 400$ with eq. (8a) or $K = 200$ with eq. (8c). However, $S/S_{FG} = 0.83$ and 0.92 for those cases, respectively. The point is that there are at least two unknowns, $W_c(\rho)$ and $W_T(\rho, T)$ or P_c and P_T . Eq. (3) can be used to determine $\rho(E)$ from data once $P(E) = P_c + P_T$ is deduced from jet analysis⁵. If eq. (9) is assumed to hold with $\alpha = 2/3$, then $W_T(E)$ could be deduced knowing $S(E)$ from composition analysis^{15,16,21} and $\rho(E)$. In this idealized scenario, eq. (2) would give, finally, $W_c(\rho)$ for $\rho = \rho(E)$. Of course, even in this idealized scenario, very high precision measurements ($\lesssim 10\%$ accuracy) must be made of both $P(E)$ and $S(E)$ in order to map out $W_c(\rho)$.

We now are in the position to see why the calculations of Refs. (10,13,15,18-20) were so insensitive to variations in the equation of state. First numerical uncertainties were typically on the order of $\sim 50\%$ in 3D hydrodynamical calculations. At that level we have little hope to observe the expected 30% effects from eqs. (3,9). Second, calculations

have concentrated up to now on the higher energy region $E \gtrsim 250$ MeV/nucleon. The most extensive comparisons with data have been made for Ne + U at $E = 400$ MeV/nucleon^{9,10,20,21}. As seen in Fig. 1, there is significantly less sensitivity to W_c at these energies than around $E \sim 100$ MeV/nucleon.

Knowing the accuracy ($\lesssim 10\%$) in measurements of $P(E)$ and $S(E)$ that are necessary in order to map out a "normal" $W_c(\rho)$, we confront finally the question of whether such precision measurements are realistic at this time. Up to now we have purposely considered the most optimistic scenario in which $P(E)$ and $S(E)$ follow from eq. (1). There are, however, several obvious complications. First, hydrodynamics may apply only to a fraction of the interaction zone, where multiple collisions lead to rapid, local thermal equilibrium. Finite number and nonequilibrium effects¹¹ must be subtracted in determining $P(E)$ and $S(E)$ from data. An important step in this direction will be to scatter the heaviest nuclei, U + U, to reduce such effects. Second, the jetting phenomena predicted in hydrodynamics^{4,5} must be firmly established if $P(E)$ is ever to be determined experimentally. We note that intranuclear cascade calculations²⁶ have predicted for light nuclei as Ar + Ar a much smaller perpendicular momentum transfer to the spectator nucleons than calculated in hydrodynamics^{4,5}. There is already evidence (the forward suppression of protons in the high multiplicity triggered Ne + U, 400 MeV/nucleon data¹) that nuclear collisions are less transparent than expected from intranuclear cascade models. However, the crucial test for hydrodynamics will be the jet analysis (triple differential cross sections)⁵. If, indeed, clear hydrodynamic phenomena are established (especially U + U at $E \sim 100$ MeV/nucleon), we can proceed to

the next step of composition analysis^{15,16,21}. Fitting the d/p , α/p , π/p ratios as well as their energy spectra determines¹⁶ $S(E)$ if chemical equilibrium and isentropic expansion were valid in nuclear collisions. Estimates²⁷ via the Navier-Stokes equation for the additional entropy, ΔS , produced in the expansion phase show that $\Delta S/S \sim 0.2$. The isentropic assumption is therefore not bad, but the sensitivity required ($\Delta S/S \lesssim 0.1$) to distinguish various (reasonable) equations of state lies within the noise of such effects. Therefore, the $S(E)$ obtained via the Euler equation¹⁵ cannot be used to compare with data yet. Full 3D Navier-Stokes equations must eventually be solved to high accuracy²². Experimentally, measurement of the A dependence of $S(E)$ is necessary to help untangle viscosity and thermal conductivity effects from shock heating. Simple estimates²⁷ indicate, for example, that ΔS decreases as $\sim A^{-1/3}$. The question of chemical equilibrium still needs much further study. Calculations using hadron chemistry equations¹⁷ cast doubt on full chemical equilibration. Furthermore, not every species is likely to be equilibrated to the same degree. Ideally, hadron chemistry calculations in 3D Navier-Stokes equations would be necessary to answer this question.

We conclude that probing the properties of dense nuclear matter via nuclear collisions is a challenging but formidable task. We have found that an accuracy on the order of 10% will be required for $P(E)$ and $S(E)$ in order to deduce $W(\rho, T)$ from data. High precision data on triple differential cross sections for p, d, α , involving 4π exclusive event shape analysis, will be necessary to carry out the program of jet analysis⁵ and composition analysis^{15,16,21}. At the same time, rather elaborate theoretical calculations of equal precision will be required to analyze that data in terms of $P(E)$ and $S(E)$. The prize, $W(\rho, T)$, is certainly worth the effort.

Acknowledgments

We acknowledge stimulating discussions with G. Bertsch, J. Kapusta, J.R. Nix, A. Sierk, and D. Strottman.

This work was supported by the Director, Office of Energy Research, Division of Nuclear Physics of the Office of High Energy and Nuclear Physics of the U.S. Department of Energy under Contract W-7405-ENG-48 and by Deutscher Akademischer Austausch Dienst (DAAD), Bonn, West Germany.

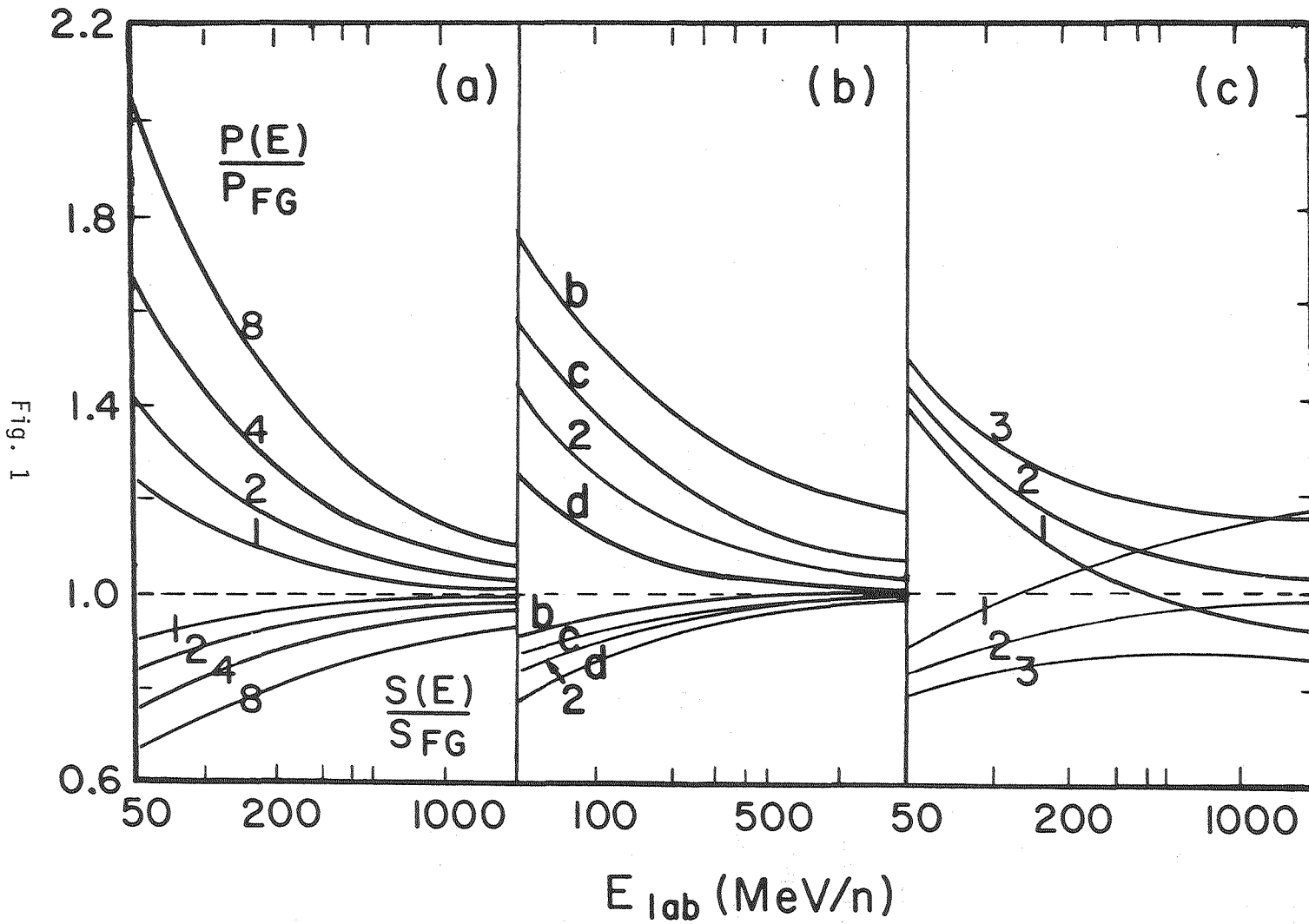
References:

1. R. Stock, et al., Phys. Rev. Lett. 44 (1980) 1243.
2. H.G. Baumgardt, et al., Z. Physik A237 (1975) 359
and J. Phys. G (1979) L231.
3. H.H. Gutbrod, LBL-preprint 11123.
4. H. Stöcker, J.A. Maruhn, and W. Greiner, Phys. Rev. Lett. 44 (1980)
725 and Z. Phys. A293 (1979) 173.
5. H. Stöcker, et al., LBL-preprint 11774 and GSI-preprint 80-9.
6. W.G. Meyer, H.H. Gutbrod, Ch. Lukner, and A. Sandoval, Phys. Rev. C22
(1980) 179.
7. A.I. Warwick, et al., and R. Renfordt, et al., talks presented at the
Asilomar meeting on 4π physics, February 8-11, 1981.
8. H. Stöcker and B. Müller, GSI-preprint 80-4.
9. J.R. Nix, Prog. Part. Nucl. Phys. 2 (1979) 237.
10. H. Stöcker, J. Hofmann, J.A. Maruhn, W. Greiner,
Prog. Part. Nucl. Phys. 4 (1980) 133.
11. J. Randrup, Nucl. Phys. A316 (1979) 509;
J. Knoll and J. Randrup, Nucl. Phys. A324 (1979) 445.
12. S. Nagamiya, et al., Phys. Lett. 81B (1979) 147;
I. Tanihata, et al., Phys. Lett. 97B (1980) 363.
13. P. Danielewicz, Nucl. Phys. A314 (1979) 465.
14. H. Stöcker, J.A. Maruhn, and W. Greiner, Phys. Lett. 81B (1979) 303
and Z. Physik A286 (1978) 121.
15. J.I. Kapusta and D. Strottman, Preprint LA-UR-80-1831 (1980).
16. P.J. Siemens and J.I. Kapusta, Phys. Rev. Lett. 43 (1979) 1486;
I.M. Mishustin, F. Myhrer and P.J. Siemens, Phys. Lett. 95B (1980)
361.

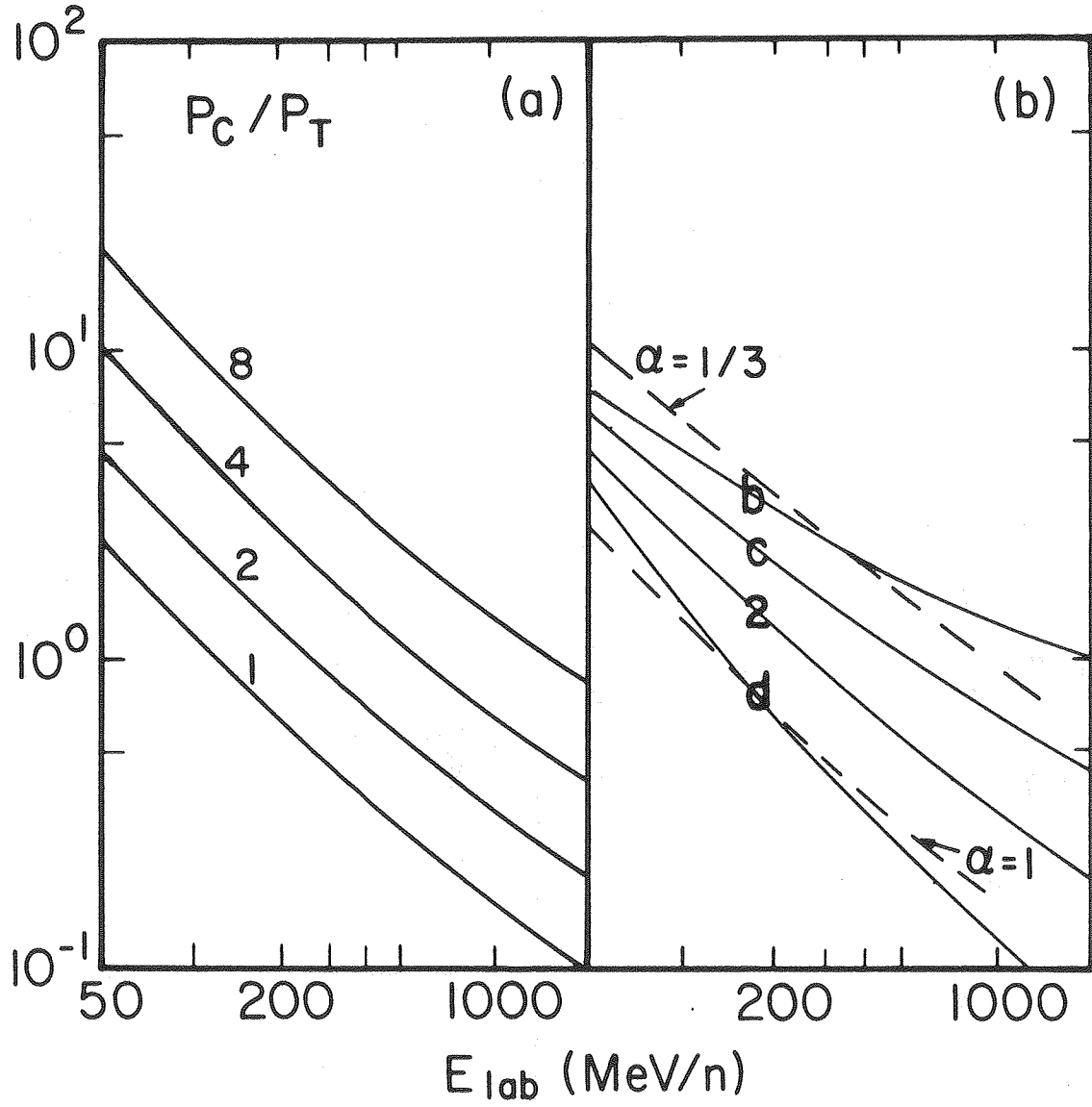
17. I. Montvay and J. Zimanyi, Nucl. Phys. A312 (1979) 490.
18. G. Bertsch and A. Amsden, Phys. Rev. C18 (1978) 1293.
19. A.J. Sierk and J.R. Nix, Phys. Rev. C22 (1980) 1920.
20. J.R. Nix and D. Strottman, Preprint LA-UR-80-814 (1980).
21. L.P. Csernai, et al., University Frankfurt preprint 38-80, to be published; J.A. Maruhn, et al., GSI-Report 5-80, to be published; M. Gyulassy, Nucl. Phys. A354 (1981) in press; LBL-11790 preprint (1980).
22. G. Buchwald, et al., Univ. Frankfurt preprint 42-80, to be published.
23. J.D. Walecka, Ann. Phys. 83 (1974) 491; Phys. Lett. 59B (1975) 109.
24. J. Boguta and A.R. Bodmer, Nucl. Phys. A292 (1977) 413.
25. H. Stöcker, R.Y. Cusson, J.A. Maruhn, and W. Greiner, Z. Physik A294 (1980) 125 and GSI preprint 80-18.
26. J. Cugnon and S.E. Koonin, Cal Tech MAP-17 preprint (1980).
27. L.P. Csernai and H.W. Barz, Z. Phys. A296 (1980) 1.

Figure Captions

1. The ratio of $P(E)$ to P_{FG} , eqs. (3,7), upper curves, and $S(E)$ to S_{FG} , eqs. (9,10), lower curves, are shown as a function of lab kinetic energy per nucleon for a variety of equations of state.
 - a) $K = 100, 200, 400, 800$ MeV for curves 1, 2, 4, 8, respectively, assuming W_c given by Eq. (8a) and $\alpha = 2/3$ for P_T .
 - b) $K = 200$ MeV and $\alpha = 2/3$ fixed but W_c given by eqs. (8a-d), curves 2, b, c, d, respectively.
 - c) $K = 200$ MeV, eq. (8a) fixed but $\alpha = 1/3, 2/3, 1$ for curves 1, 2, 3, respectively.
2. The ratio of the compression to thermal pressures, P_c/P_T as a function of energy corresponding to $W(\rho,T)$ used in Fig. 1 respectively.
3.
 - a) Total pressure $P(E)$ vs E for Fermi gas (solid line) compared with mean field theory, $K = 550$ from Ref. 23, $K = 270$, and $K = 170$ (marked with X) from Ref. 24.
 - b) Entropy per baryon $S(E)$ vs E for equations of state in (a). S_{FG} is the exact Fermi gas result.
 - c) The maximum density, $\rho(E)$ vs E for equations of state in Fig. 1b. [FG = eq. (6), $\alpha = 1/3$ is for curve 1 of Fig. 1c].

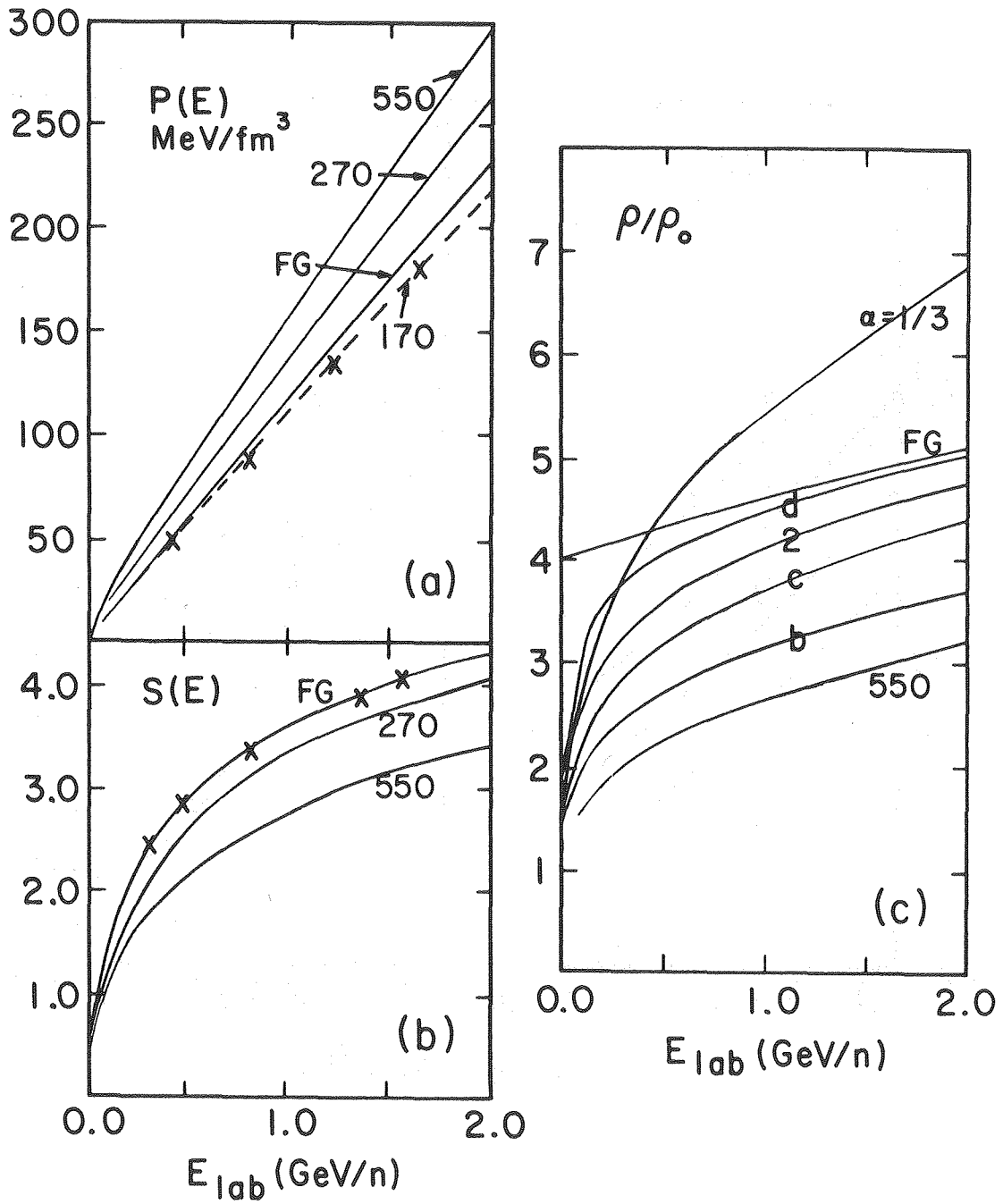


XBL 813-8434



XBL 813-8435

Fig. 2



XBL 813-8436

Fig. 3